Charge Transport and Recombination in Polyspirobifluorene Blue Light-Emitting Diodes

Nicolai, Herman T.; Hof, Andre; Oosthoek, Jasper L. M.; Blom, Paul W. M.

Published in:
Advanced Functional Materials

DOI:
10.1002/adfm.201002293

Publication date:
2011

Charge Transport and Recombination in Polyspirobifluorene Blue Light-Emitting Diodes

*Herman T. Nicolai, André Hof, Jasper L. M. Oosthoek, and Paul W. M. Blom**

The charge transport in blue light-emitting polyspirobifluorene is investigated by both steady-state current-voltage measurements and transient electroluminescence. Both measurement techniques yield consistent results and show that the hole transport is space-charge limited. The electron current is found to be governed by a high intrinsic mobility in combination with electron traps. Numerical simulations on light-emitting diodes reveal a shift in the recombination zone from the cathode to the anode with increasing bias.

1. Introduction

In recent decades, polymer light-emitting diodes (PLEDs) have been the subject of intensive research due to their potential for low cost fabrication.[1,2] Understanding the device operation of PLEDs is crucial for the improvement of device performance. PLEDs nowadays have started to emerge in display applications and they are also considered as interesting candidates for lighting applications. Efficient blue emitters are essential for the realization of such applications. Polyfluorenes are attractive blue emitters due to their high photoluminescence efficiency and wide band gap.[3,4] They can be considered as a type of polyphenylene where pairs of phenylene rings are connected by an additional carbon atom, named the C-9 atom, keeping the phenyl rings in plane and resulting in improved conjugation. Additionally, the C-9 atom allows for easy substitution of side chains to tune the solubility and interchain interactions without affecting the electronic structure.[5–7] The first polyfluorene PLED was reported by Yoshino et al.[8,9] The material suffered from a low molecular weight and a poor device performance. Since then, considerable progress has been made in the synthesis of polyfluorene derivatives and the performance of polyfluorene devices. Highly efficient PLEDs were achieved by copolymerizing fluorene with suitable units to tailor the electric and optical properties.[10–14] Salbeck et al. introduced spiro centers in fluorene compounds[15,16] and in fluorene polymers.[17] The spiro center links two fluorene units by connecting them at the C-9 atom while the planes of the fluorene units are oriented perpendicular to each other. This spiro linkage significantly increases the glass transition temperature (T_g) and thus improves the morphological stability while also minimizing unwanted long wavelength emission.[18]

A critical issue for the efficiency of PLEDs is the charge balance. Polyfluorene PLEDs have been reported to exhibit an unbalanced charge transport and to be dominated by electrons.[10,19] However, polyfluorene derivatives often have a high ionization potential resulting in an injection barrier for holes.[20] It is therefore not always clear whether the unbalanced transport is the result of an intrinsic unbalanced charge transport or the result of an unbalanced charge injection. To improve the injection and conduction of holes in polyfluorene derivatives, triarylamines are commonly used, which are known to be good hole conductors.[21,22] Redecker et al. reported mobilities up to 3×10^{-7} m^2 V^{-1} s^{-1} in a fluorene copolymerized with triarylamine.[23] The triarylamines were mentioned to lower the ionization potential of the copolymer and thus improve the hole injection. In addition to copolymerization in the main chain, the triarylamine units may also be used as end-capping[19] or connected to the C-9 atom of the fluorene unit.[24] The device operation of such a copolymer-based PLED is more complicated than for the conventional PLEDs based on for example poly(*p*-phneylene vinylene) (PPV) derivatives. In PPV the mobilities of electrons and holes are identical,[25] facilitating the understandingof the trap-limited electron transport, since the intrinsic trap-free mobility can be obtained from the hole transport.[26] In a copolymer, however, the hole transport is modified by the presence of the triarylamine units, such that the hole and electron mobility are not necessarily equal. In order to disentangle the various processes we study the charge transport of a blue-emitting polyspirobifluorene copolymer by both steady-state current-voltage (*J*–*V*) and time-resolved electroluminescence measurements. The polyspirobifluorene polymer studied is a copolymer containing 3 monomers including a triarylamine-biphenyl hole transport unit (shown in **Figure 1**) and functions as the blue backbone material for a white emitting copolymer described elsewhere.[27–30] A detailed understanding of the charge transport in the blue backbone polymer is a prerequisite for the understanding of the device operation of the white light emitting diode.

H. T. Nicolai, Dr. A. J. Hof, J. L. M. Oosthoek, Prof. P. W. M. Blom
Molecular Electronics
Zernike Institute for Advanced Materials
University of Groningen
Nijenborgh 4, NL-9747AG Groningen, The Netherlands
E-mail: p.w.m.blom@rug.nl
Prof. P. W. M. Blom
Holst Centre
High Tech Campus 31, NL-5605KN Eindhoven, The Netherlands

DOI: 10.1002/adfm.201002293

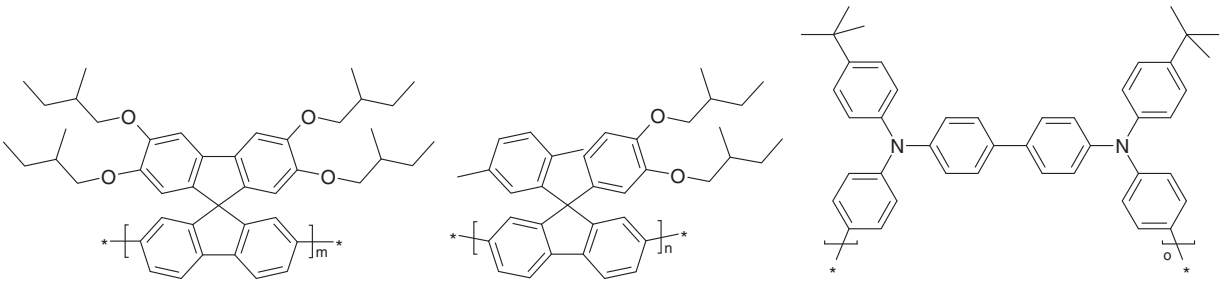

Figure 1. Chemical structure of the blue emitting polyspirobifluorene copolymer studied. The composition of the copolymer is m = 50%, n = 40%, o = 10%.

2. Results and Discussion

PLEDs of the polyspirobifluorene were fabricated and characterized by steady-state and transient measurements. For an optimal device performance the electron current and hole current need to be balanced to ensure that the recombination is located at the center of the active layer. A recombination zone that is located close to the contacts results in quenching and a loss of efficiency.[31] In addition to the PLEDs, single carrier devices have also been fabricated to measure the electron current and hole current independently. The devices consisted of a polymer layer sandwiched between two electrodes. The double carrier devices consisted of a layer of patterned indium tin oxide (ITO) with a spincoated layer of poly(3,4-ethylenedioxythiophene):poly(4-styrene sulphonate) (PEDOT:PSS) as the anode and an evaporated layer of Ba/Al functioned as the cathode. Hole-only devices were fabricated by using a Pd/Au as a cathode instead of Ba/Al to block the electron injection. By using a hole blocking anode consisting of Al, electron-only devices were fabricated.[26,32]

2.1. Steady-State Current–Voltage Measurements

The *J*–*V* curves of the hole-only devices showed a voltage and thickness dependence indicative of a space-charge limited hole current. The zero-field mobility can then be obtained directly from the *J*–*V* characteristics using the Mott–Gurney law[33]

$$J = \frac{9}{8}\varepsilon_0\varepsilon_r\mu\frac{(V - V_{bi})^2}{L^3} \quad (1)$$

where $\varepsilon_0\varepsilon_r$ is the dielectric constant, μ_0 the zero-field mobility, V the applied voltage, L the active layer thickness, and V_{bi} the built-in voltage arising from the difference in workfunctions between anode and cathode. The value of V_{bi} can be identified in an *J*–*V* curve as the voltage at which the current starts to deviate from the exponential diffusion current,[34] and was determined at V_{bi} = 1.3 V. An equal built-in voltage has been observed for a similar polyfluorene derivative.[35] A relative dielectric constant of 3.1 was obtained from impedance spectroscopy measurements. The room temperature hole mobility at low electric fields and low carrier densities was determined to be $\mu_0 \sim 1 \times 10^{-11}$ m^2 V^{-1} s^{-1}. In contrast to the hole current, the electron-only devices exhibited steep *J*–*V* curves with a strong dependence on the polymer layer thickness, indicative of trap-limited conduction with an exponential energy distribution of traps, as has also been observed for PPV derivatives.[36] In that case, the electron current can be expressed analytically as[37]

$$J = N_c q\mu_n\left(\frac{\varepsilon_o\varepsilon_r}{q N_t}\right)^r\left(\frac{2r+1}{r+1}\right)^{r+1}\left(\frac{r}{r+1}\right)^r\frac{V^{r+1}}{L^{2r+1}} \quad (2)$$

with q the elementary charge, N_c the effective density of states, μ_n the free electron mobility, N_t the amount of traps, and $r = T_t/T$, where T_t is the characteristic temperature of the exponential distribution. The magnitude of a trap-limited current depends on the mobility of the free charge carriers as well as the amount and energy distribution of the traps. From *J*–*V* measurements only it is therefore not possible to independently determine the mobility of the free carriers and the amount of traps. For PPV derivatives, it has been demonstrated that the electron mobility is equal to the hole mobility by passivating the electron traps with the n-type dopant dimethylcobaltocene.[25] A similar result was obtained by Chua et al. who reported similar intrinsic mobilities of electrons and holes in transistors.[38] However, for the polyspirobifluorene polymer studied here, the hole transport is governed by the presence of triarylamine-biphenyl hole transporting units,[39,40] which makes such an assumption questionable. As a result, Equation 2 can only be used to obtain an estimate for T_t from the thickness dependence of the polyspirobifluorene electron current, which yielded T_t = 1750 K.

Figure 2 shows the electron-, hole- and double carrier current at room temperature for a polymer thickness of $L \sim 180$ nm. A cross-over point in the *J*–*V* curves of the hole current and electron current is observed, suggesting that the double carrier device is dominated by holes below a voltage of V–V_{bi} = 9 V, and dominated by electrons above this voltage where the electrons traps become filled. This cross-over already indicates that the intrinsic trap-free electron-mobility must be higher than the hole mobility. **Figure 3** shows the normalized current efficiency (light output/current) of the PLED. The current efficiency increases up to a maximum value at a bias of V–V_{bi} = 5 V above the built-in voltage, after which it slowly decreases with increasing bias.

2.2. Transient Electroluminescence

To obtain an independent measure for the electron mobility transient electroluminescence (TEL) measurements were

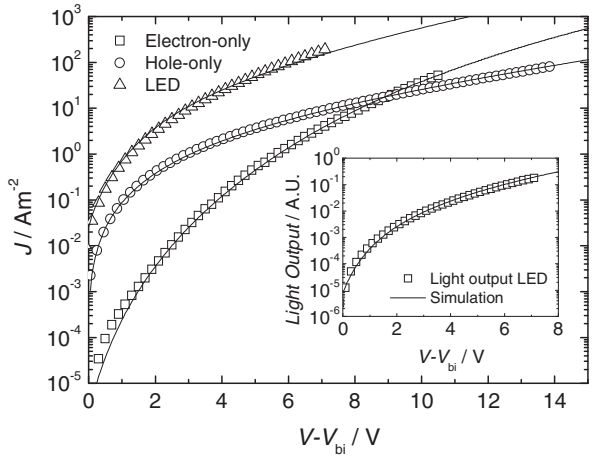

Figure 2. *J–V* characteristics of hole-only, electron-only, and double carrier devices with an active layer thickness of ~180 nm. There is a cross-over point between the *J–V* curves of the hole-only device and the electron-only device at $V–V_{bi} = 9$ V. Solid lines represent the modeling results. The inset shows the light output of the PLED and the simulation.

performed.[41,42] This measurement technique is based on the delay time between the application of a voltage pulse and the onset of light emission. When a voltage is applied to the PLED charges are injected from both electrodes and travel towards each other driven by the electric field. When the two types of charges meet, an exciton can be formed which can decay radiatively. Due to the time required for the charge carriers to travel towards each other, there is a delay between the application of a voltage pulse and the onset of light emission. Assuming that one of the two charge carrier types is dominant, this time delay represents the transit time through the polymer layer for the fastest charge carrier type. The transient mobility can then be calculated using

$$\mu = \frac{L^2}{\tau \left(V_{\text{pulse}} - V_{\text{bi}}\right)} \tag{3}$$

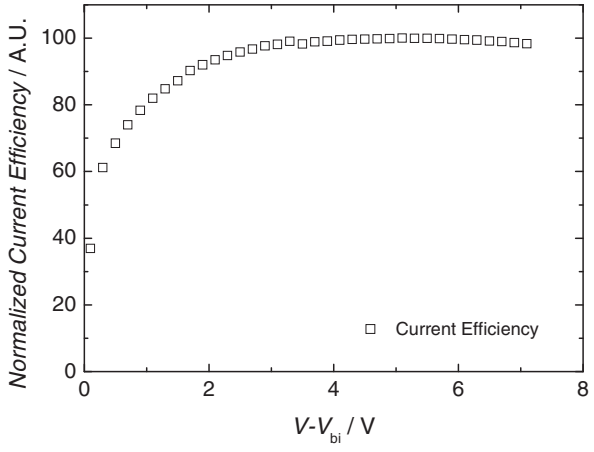

Figure 3. Normalized current efficiency of a PLED with an active layer thickness of 180 nm. The current efficiency increases with increasing bias up to a maximum at $V–V_{bi} = 5$ V.

with L the active layer thickness, V_{pulse} the voltage pulse height, and V_{bi} the built-in voltage. A sensitive method to measure the delay time at low light intensities is to apply a voltage pulse train with an increasing pulse width to the PLED and then to measure the integrated light emission.[43] If the pulse width is too short, the charges do not have enough time to reach each other and no light emission will be detected. When the pulse width is long enough, light emission will occur, and the integrated light-output scales linearly with the pulse width. By extrapolating this linear regime to small pulse width, a measure for the delay time τ can be obtained. Since light output is required for a TEL measurement, this technique can only be employed on double carrier devices and it is therefore not known a priori which type of charge carrier determines the transit time and the measured mobility. To distinguish whether the measured transit times originate from electrons or holes, double layer devices have been fabricated, consisting of the polymer layer and a thin ($L \sim 40$ nm) layer of the oligomer *p*-Bis(*p*-styrylstyryl)benzene (OPV5). This oligomer can be evaporated and is insoluble in toluene, allowing it to be deposited either before or after spincoating of the polymer layer. The highest occupied molecular orbitals (HOMO) of a polymer similar to the polyspirobifluorene investigated here was estimated to be ~5.3 eV[39] while the HOMO of OPV5 is estimated at ~5.4 eV.[44] The HOMO levels of both materials are therefore expected to align relatively well. As a result there is no significant injection barrier for holes expected when a thin OPV5 layer is deposited between the anode and the polyspirobifluorene layer. Indeed, we observe that such an additional OPV5 layer of 40 nm gives rise to an approximately equal device current as the 200 nm single layer PLED (**Figure 4**), in spite of the increased total layer thickness. This confirms the absence of an injection barrier of holes. The OPV5 oligomer has a smaller band gap (2.6 eV) than the blue-emitting

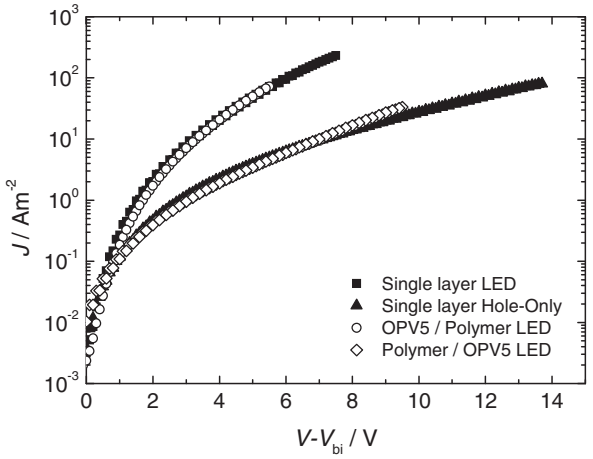

Figure 4. *J–V* characteristics of single and double layer devices. The single layer devices have an active polymer layer thickness of 200 nm, the double layer devices have a polymer layer thickness of 200 nm with an additional 40 nm OPV5 layer either between the polymer layer and the cathode, or between the polymer layer and the anode. The inclusion of the OPV5 layer between the anode and the polymer layer does not significantly affect the device current. The inclusion of the OPV5 layer between the polymer and the cathode lowers the device current to the level of the polymer hole-only device.

polyspirobifluorene (3.1 eV), emitting yellow light. An injection barrier for electrons is therefore expected when the OPV5 layer is placed on top of the polymer layer. In Figure 4, it is demonstrated that for this case, the double carrier current is reduced to the level of the single layer hole-only device. This clearly shows that the electron injection into the polymer layer is now suppressed to such an extent that the device current is completely dominated by holes.

Figure 5 shows the transient mobilities obtained from TEL measurements on single layer and double layer LEDs with the OPV5 layer in between the polymer layer and the cathode. In the double layer PLED, the electrons face an injection barrier at the OPV5/polymer interface and accumulate in the OPV5 layer. Holes have to travel through the polymer layer and recombine with electrons in the OPV5 layer. The yellow emission from this double layer device confirms that the recombination in these double layer devices indeed takes place in the OPV5 layer. As a result, the TEL measurements in a double layer device reflect the transport properties of holes in the polyspirobifluorene. We observe that the transient mobility of the double layer device is approximately one order of magnitude lower than the transient mobility of the single layer polyspirobifluorene PLED. This clearly demonstrates that the faster transit times of the single layer devices must originate from the electron transport. The hole mobilities measured in the double layer devices extrapolate to a zero-field mobility of ~10^{-11} m^2 V^{-1} s^{-1} which is in agreement with the zero-field mobility obtained from the steady-state *J–V* measurements. The electron mobility as measured in the single layer device is one order of magnitude larger than the hole mobility and extrapolates to a zero-field mobility of ~10^{-10} m^2 V^{-1} s^{-1}. The higher electron mobility as observed in these TEL measurements is also in agreement with the cross-over of the hole- and electron current (Figure 2), showing a better electron transport once sufficient traps are filled.

2.3. Numerical Modeling

The mobilities obtained by the TEL measurements on the single-carrier devices serve as input to model the electrical characteristics of the light-emitting diode. We apply a numerical device model which solves the continuity and Poisson equations using an iterative scheme.[45] The model takes into account both drift and diffusion of charge carriers, a density dependent mobility,[46] and recombination of the Langevin-type.[47] The electric field and density dependence of the hole mobility is governed by 3 parameters: the site spacing a, the width of the Gaussian distribution of density of states σ and a prefactor for the mobility μ_0^*, which defines the mobility in the limit of zero density, zero electric field and infinite temperature.[48] The temperature and thickness dependence (**Figure 6**) of the hole current could be consistently modeled using the fit parameters: $\mu_0^* = 750$ m^2 V^{-1} s^{-1}, $a = 1.5$ nm and $\sigma = 0.15$ eV. At low electric field and low charge carrier densities, these parameters yield a mobility in the order of 10^{-11} m^2 V^{-1} s^{-1} which agrees well with the zero-field mobility found using Equation 1. The found value of σ is higher than reported for other arylamine containing polyfluorenes[35,49] which suggests that the polymer studied here has a larger energetic disorder.

As shown above, the transient electron mobility was found to be approximately one order higher than the transient hole mobility. However, the question still arises as to whether the measured transient electron mobility is an *effective* mobility, which is influenced by the presence of electron traps. The temperature, thickness, and voltage dependence of the electron current can be consistently described by the parameters: $\mu_0^* = 1000$ m^2 V^{-1} s^{-1}, $a = 2.0$ nm and $\sigma = 0.12$ eV for the free electron mobility, in combination with an exponential electron trap distribution with a trap density $N_t = 6.5 \times 10^{23}$ m^{-3} and $T_t = 1750$ K (**Figure 7**). The resulting free electron mobility at room temperature and low fields is one order of magnitude larger than the measured transient mobility. This is likely due to the fact that the parameters used to model the *J–V* characteristics describe

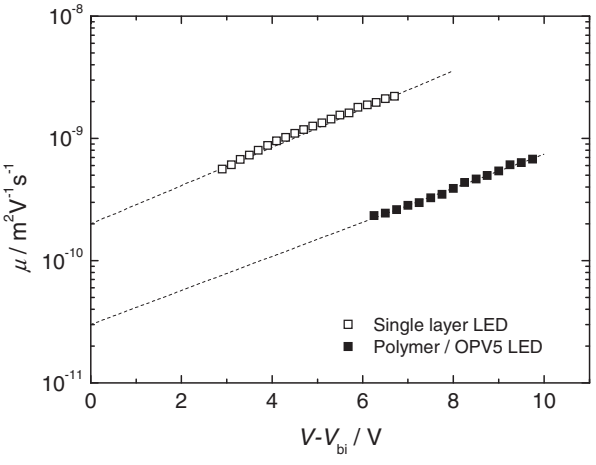

Figure 5. Transient mobility of single and double layer devices with a polymer layer thickness of 200 nm. The transient mobility of the double layer device (dominated by the holes transport) is one order of magnitude lower than the transient mobility of the single layer device (dominated by electron transport).

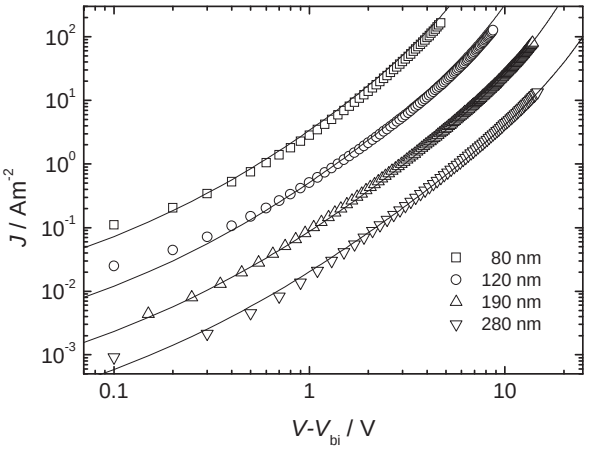

Figure 6. *J–V* characteristics and simulation of hole-only devices with different thicknesses. The hole transport can be modeled with one set of parameters, $\mu_0^* = 750$ m^2 V^{-1} s^{-1}, $a = 1.5$ nm, and $\sigma = 0.15$ eV.

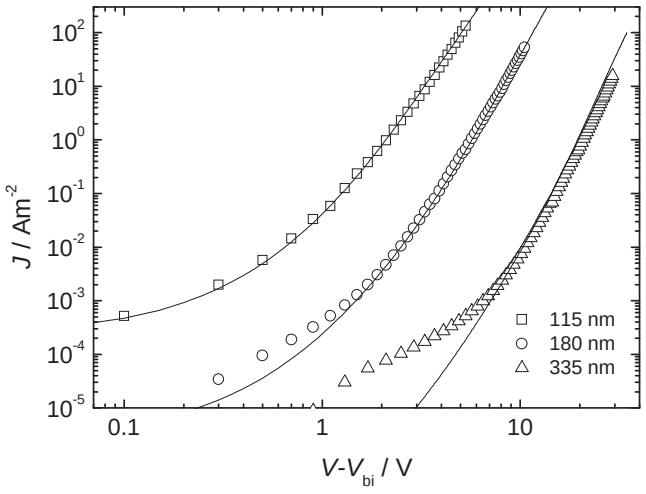

Figure 7. *J–V* characteristics and simulation of electron-only devices with different thicknesses. The electron transport can be modeled with the mobility parameters $\mu_0^* = 1000$ m^2 V^{-1} s^{-1}, $a = 2.0$ nm, and $\sigma = 0.12$ eV, with the inclusion of electron traps distributed exponentially in energy, characterized by $N_t = 6.5 \times 10^{23}$ m^{-3} and $T_t = 1750$ K.

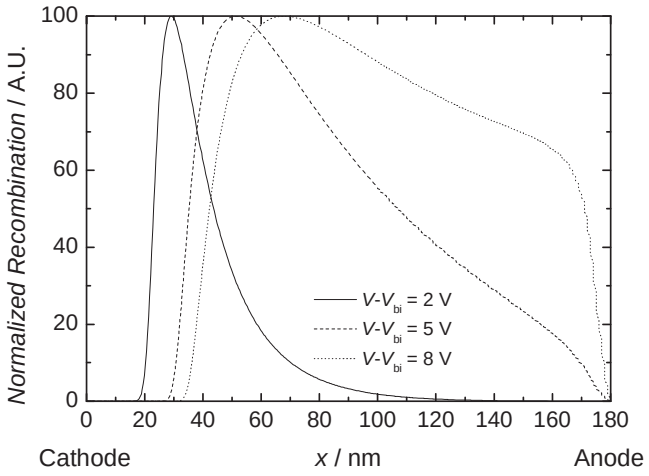

Figure 8. Distribution of the recombination zone in the PLED. A shift in the location of the recombination zone is observed with increasing bias. At higher bias, the recombination shifts away from the cathode.

the intrinsic trap-free electron mobility, in contrast to the trapping-dependent transient mobility.

By combining the parameters for the hole and electron transport, the double carrier device can be modeled (Figure 2). The numerical calculations carried out on the polyspirobifluorene based PLED provide insight into internal quantities that are otherwise inaccessible, such as the distribution of the electric field and the concentration profiles of the electrons and holes. Of direct relevance for the quantum efficiency, as well as to the outcoupling efficiency of the generated excitons, is the position of the recombination zone inside the PLED. In PPV-based PLEDs, it has been demonstrated that the recombination zone is located close to the cathode due to the poor electron transport, leading to quenching of the excitons at the metallic cathode.[50] With increasing bias voltage, the distribution moves on average slightly away from the cathode, giving rise to an increase of the efficiency. In the polyspirobifluorene PLEDs, as shown in **Figure 8**, the recombination zone shifts completely from the cathode towards the anode with increasing bias. This is due to the combination of a relative low hole mobility, a relative high electron mobility and the presence of electron traps.

As shown in Figure 2, at low bias voltage the PLED is hole dominated and the recombination zone is located at the cathode. For sufficiently high bias voltage, the electron traps are filled and the electron currents passes the hole current due to the higher mobility of the free electrons. In that case, the recombination is shifted towards the anode. At an intermediate bias of $V - V_{bi} = 5$ V, the recombination zone is relatively spread out in the center of the active layer. This point corresponds exactly to the maximum in the current efficiency as shown in Figure 3. This shows that the dependence of the current efficiency on voltage is the result of the shift of the recombination zone. The maximum efficiency is obtained at the voltage where the best combination is obtained between reduced quenching losses at the electrodes and an enhanced outcoupling. The average distance of the recombination profile from the cathode amounts to 50 nm for the blue-emitting polyspirobifluorene PLED.

3. Conclusions

The charge transport in polymer PLEDs based on a blue-emitting polyspirobifluorene derivative has been investigated. Steady-state current voltage measurements and TEL measurements both show that the intrinsic electron mobility is significantly larger than the hole mobility, but the electron current is reduced by the presence of electron traps. The combination of a high intrinsic electron mobility with the presence of electron traps results in a cross-over point in the *J–V* curves of the electron current and the hole current. For the PLED, this leads to a large shift of the recombination zone depending on the applied voltage. Ideally, the recombination zone is located in the emissive layer where the quenching at the electrodes is minimized and the optical outcoupling is maximized. To optimize the performance of the PLED, it is therefore necessary to tune the mobilities of the electrons and holes such that the recombination is located at typically 50 nm away from the cathode.

4. Experimental Section

PLEDs and single carrier devices were fabricated on glass substrates with a patterned ITO layer. The substrates were cleaned, dried, and treated with UV-ozone. A layer of PEDOT:PSS (Clevios P VP Al 4083 supplied by H. C. Starck) was spincoated from solution and baked (140 °C). The typical thickness of the PEDOT:PSS layer was 60 nm. The polymer layers were spincoated in a nitrogen atmosphere from a toluene solution. The OPV5 layer and the cathodes were deposited by thermal evaporation (chamber pressure ca. 10^{-6} mbar). Electron-only devices were fabricated on glass substrates with an Al anode (30 nm). For the electron-only devices and the LEDs, the cathode consisted of a Ba layer (5 nm) and an Al capping layer (100 nm). For the hole-only devices, the cathode consisted of a Pd layer (20 nm) followed by an Au capping layer

(80 nm). The devices were characterized in a nitrogen atmosphere using a computer controlled Keithley 2400 SourceMeter.

Acknowledgements

The authors thank Margreet de Kok (Philips Research) for helpful discussions and suggestions. We thank the European Commission for funding of this work under contract IST-004607 (OLLA). The authors acknowledge Merck KGaA for the supply of the polymer.

Received: October 30, 2010
Revised: December 9, 2010
Published online: March 1, 2011

[1] J. H. Burroughes, D. D. C. Bradley, A. R. Brown, R. N. Marks, K. Mackay, R. H. Friend, P. L. Burns, A. B. Holmes, *Nature* **1990**, *347*, 539–541.
[2] R. H. Friend, R. W. Gymer, A. B. Holmes, J. H. Burroughes, R. N. Marks, C. Taliani, D. D. C. Bradley, D. A. D. Santos, J. L. Bredas, M. Logdlund, W. R. Salaneck, *Nature* **1999**, *397*, 121–128.
[3] Q. Pei, Y. Yang, *J. Am. Chem. Soc.* **1996**, *118*, 7416–7417.
[4] A. W. Grice, D. D. C. Bradley, M. T. Bernius, M. Inbasekaran, W. W. Wu, E. P. Woo, *Appl. Phys. Lett.* **1998**, *73*, 629–631.
[5] D. Neher, *Macromol. Rapid Commun.* **2001**, *22*, 1365–1385.
[6] S. A. Chen, H. H. Lu, C. W. Huang, *Adv. Polym. Sci.* **2008**, *212*, 49–84.
[7] R. Abbel, A. P. H. J. Schenning, E. Meijer, *J. Polym. Sci., Part A: Polym. Chem.* **2009**, *47*, 4215–4233.
[8] M. Fukuda, K. Sawada, K. Yoshino, *Jpn. J. Appl. Phys.* **1989**, *28*, L1433-L1435.
[9] Y. Ohmori, M. Uchida, K. Muro, K. Yoshino, *Jpn. J. Appl. Phys.* **1991**, *30*, L1941-L1943.
[10] M. Inbasekaran, E. Woo, W. Wu, M. Bernius, L. Wujkowski, *Synth. Met.* **2000**, *111–112*, 397–401.
[11] B. Liu, W. Yu, Y. Lai, W. Huang, *Chem. Mater.* **2001**, *13*, 1984–1991.
[12] P. Herguth, X. Jiang, M. S. Liu, A. K. Jen, *Macromolecules* **2002**, *35*, 6094–6100.
[13] E. Lim, B. Jung, H. Shim, *Macromolecules* **2003**, *36*, 4288–4293.
[14] W. Wu, M. Inbasekaran, M. Hudack, D. Welsh, W. Yu, Y. Cheng, C. Wang, S. Kram, M. Tacey, M. Bernius, R. Fletcher, K. Kiszka, S. Munger, J. O'Brien, *Microelectron. J.* **2004**, *35*, 343–348.
[15] J. Salbeck, N. Yu, J. Bauer, F. Weissörtel, H. Bestgen, *Synth. Met.* **1997**, *91*, 209–215.
[16] F. Steuber, J. Staudigel, M. Stössel, J. Simmerer, A. Winnacker, H. Spreitzer, F. Weissörtel, J. Salbeck, *Adv. Mater.* **2000**, *12*, 130–133.
[17] *Conjugated Polymers Having Spiro Centers and Their Use As Electroluminescence Materials*, **1997**, U.S. Patent 5,621,131.
[18] W. Yu, J. Pei, W. Huang, A. J. Heeger, *Adv. Mater.* **2000**, *12*, 828–831.
[19] T. Miteva, A. Meisel, W. Knoll, H. G. Nothofer, U. Scherf, D. C. Müller, K. Meerholz, A. Yasuda, D. Neher, *Adv. Mater.* **2001**, *13*, 565–570.
[20] A. J. Campbell, D. D. C. Bradley, H. Antoniadis, *J. Appl. Phys.* **2001**, *89*, 3343–3351.
[21] M. Stolka, J. F. Yanus, D. M. Pai, *J. Phys. Chem.* **1984**, *88*, 4707–4714.
[22] C. Giebeler, H. Antoniadis, D. D. C. Bradley, Y. Shirota, *Appl. Phys. Lett.* **1998**, *72*, 2448–2450.
[23] M. Redecker, D. D. Bradley, M. Inbasekaran, W. W. Wu, E. P. Woo, *Adv. Mater.* **1999**, *11*, 241–246.
[24] C. Ego, A. Grimsdale, F. Uckert, G. Yu, G. Srdanov, K. Müllen, *Adv. Mater.* **2002**, *14*, 809–811.
[25] Y. Zhang, B. de Boer, P. W. M. Blom, *Phys. Rev. B.* **2010**, *81*, 085201–5.
[26] M. M. Mandoc, B. de Boer, P. W. M. Blom, *Phys. Rev. B* **2006**, *73*, 155205–7.
[27] H. Becker, E. Breuning, A. Büsing, A. Falcou, S. Heun, A. Parham, H. Spreitzer, J. Steiger, P. Stössel, *Mater. Res. Soc. Symp. Proc.* **2003**, *769*, 3.
[28] C. D. Muller, A. Falcou, N. Reckefuss, M. Rojahn, V. Wiederhirn, P. Rudati, H. Frohne, O. Nuyken, H. Becker, K. Meerholz, *Nature* **2003**, *421*, 829–833.
[29] M. Gather, A. Köhnen, A. Falcou, H. Becker, K. Meerholz, *Adv. Funct. Mater.* **2007**, *17*, 191–200.
[30] M. A. Parshin, J. Ollevier, M. Van Der Auweraer, M. M. de Kok, H. T. Nicolai, A. J. Hof, P. W. M. Blom, *J. Appl. Phys.* **2008**, *103*, 113711–7.
[31] D. E. Markov, P. W. M. Blom, *Appl. Phys. Lett.* **2005**, *87*, 233511–3.
[32] R. Steyrleuthner, S. Bange, D. Neher, *J. Appl. Phys.* **2009**, *105*, 064509–8.
[33] N. F. Mott, R. W. Gurney, *Electronic Processes in Ionic Crystals*, Dover Publications, New York**1940**.
[34] V. D. Mihailetchi, P. W. M. Blom, J. C. Hummelen, M. T. Rispens, *J. Appl. Phys.* **2003**, *94*, 6849–6854.
[35] S. L. M. van Mensfoort, S. I. E. Vulto, R. A. J. Janssen, R. Coehoorn, *Phys. Rev. B* **2008**, *78*, 085208–10.
[36] M. M. Mandoc, B. de Boer, G. Paasch, P. W. M. Blom, *Phys. Rev. B* **2007**, *75*, 193202–4.
[37] P. Mark, W. Helfrich, *J. Appl. Phys.* **1962**, *33*, 205–215.
[38] L. L. Chua, J. Zaumseil, J. F. Chang, E. C. W. Ou, P. K. H. Ho, H. Sirringhaus, R. H. Friend, *Nature* **2005**, *434*, 194–199.
[39] F. Laquai, G. Wegner, C. Im, H. Bassler, S. Heun, *J. Appl. Phys.* **2006**, *99*, 023712–7.
[40] F. Laquai, D. Hertel, *Appl. Phys. Lett.* **2007**, *90*, 142109–3.
[41] S. Karg, V. Dyakonov, M. Meier, W. Riess, G. Paasch, *Synth. Met.* **1994**, *67*, 165–168.
[42] P. Ranke, I. Bleyl, J. Simmerer, D. Haarer, A. Bacher, H. W. Schmidt, *Appl. Phys. Lett.* **1997**, *71*, 1332–1334.
[43] P. W. M. Blom, M. C. J. M. Vissenberg, *Phys. Rev. Lett.* **1998**, *80*, 3819–3822.
[44] P. van Hutten, J. Wildeman, A. Meetsma, G. Hadziioannou, *J. Am. Chem. Soc.* **1999**, *121*, 5910–5918.
[45] L. J. A. Koster, E. C. P. Smits, V. D. Mihailetchi, P. W. M. Blom, *Phys. Rev. B* **2005**, *72*, 085205–9.
[46] C. Tanase, E. J. Meijer, P. W. M. Blom, D. M. de Leeuw, *Phys. Rev. Lett.* **2003**, *91*, 216601–4.
[47] M. P. Langevin, *Ann. Chim. Phys.* **1903**, *28*, 433.
[48] W. F. Pasveer, J. Cottaar, C. Tanase, R. Coehoorn, P. A. Bobbert, P. W. M. Blom, D. M. de Leeuw, M. A. J. Michels, *Phys. Rev. Lett.* **2005**, *94*, 206601–4.
[49] R. U. A. Khan, D. Poplavskyy, T. Kreouzis, D. D. C. Bradley, *Phys. Rev. B* **2007**, *75*, 035215–14.
[50] P. W. M. Blom, M. C. J. M. Vissenberg, *Mater. Sci. Eng., R.* **2000**, *27*, 53–94.